Synthesis, Conformational Studies, X-ray Structures, and Complexation Properties of Semirigid Macrocyclic Phosphonamides

Pascale Delangle,[1] Jean-Pierre Dutasta,*[,1] Luc Van Oostenryck,[2] Bernard Tinant,[2] and Jean-Paul Declercq[2]

Stéréochimie et Interactions Moléculaires, UMR CNRS 117, Ecole Normale Supérieure de Lyon, 46 allée d'Italie, F-69364 Lyon Cedex 07, France, and Laboratoire de Chimie Physique et de Cristallographie, Université Catholique de Louvain, 1 place Louis Pasteur, B-1348 Louvain La Neuve, Belgium

Received June 26, 1996[⊗]

The semirigid phosphonamide ligands **1**−**5** have been synthesized from the macrocyclic precursors **6**−**9** by reaction with 1,3-propanediol ditosylate or 1,2-dichloroethane. For the thiophosphoryl compounds **1** and **2**, and the phosphoryl derivative **5**, the reactions were carried out in biphasic aqueous NaOH solutions. The phosphoryl derivatives **3** and **4** were better obtained from NaH in anhydrous tetrahydrofuran. The conformations of the hosts in solution were deduced from low-temperature NMR and NOE difference experiments. Conformational equilibria between *exo* and *endo* forms are observed for the 18-membered macrocycles **1** and **3**. The *exo* conformer predominates in solution for the 21-membered macrocycle **2**, whereas **4** exists as rapidly exchanging conformers. The X-ray crystal structures of macrocycles **1**, **2**, and **5** have been determined as well as the complexes **1**·$Hg(SCN)_2$ and **5**·$LiNO_3$. In the Hg^{2+} complex the metal ion is located out of the macrocyclic cavity and is coordinated to the thiophosphoryl unit. In **5**·$LiNO_3$ the Li^+ cation is located inside the macrocyclic cavity and is coordinated to a tetrahedral array of oxygen donors. Free energies of complexation ($\Delta G°$) of the phosphorylated ligands **3**−**5** with alkali metal and ammonium cations were determined in $CHCl_3$ saturated with H_2O by picrate extraction experiments. The $-\Delta G°$ values are greatest for **4** complexing K^+ and NH_4^+ (7.3 and 8.0 kcal/mol, respectively). The relationships between structure and binding are discussed.

Introduction

Selective complexation of metal ions requires very efficient donor ligands that can take advantage of the chelating or, even better, the macrocyclic effect. Appropriate structural preorganization of the host molecule (the principle of preorganization) in combination with the appropriate set of complementary donor binding sites (the principle of complementarity) result in the formation of highly stable complexes with metal ions.[3] Phosphoryl derivatives such as phosphine oxides, phosphonates, and phosphates are able to form strong complexes with cationic guests and are efficient hydrogen bond acceptors. The introduction of the hard donor phosphoryl P═O group into macrocyclic structures suggests macrocyclic phosphoramides as promising ligands for alkali metal and ammonium cations. In addition, the related thiophosphoryl P═S group is capable of strong interactions with soft metal ions, although only few attempts have been made to rationally design macrocyclic hosts in which the softness of the P═S group is exploited to coordinate metal ions.

The synthesis of phosphorus-containing macrocycles, cryptands, and spherands, and the formation of their complexes are now well documented.[4] Recent representative examples in the field of phosphorus cryptands and spherands have been given by Majoral and Caminade, who developed a novel synthetic strategy using phosphodi- or trihydrazide synthons. Their approach provided a large number of interesting phosphorus macrocyclic and polymacrocyclic hosts.[5] Likewise, Whitlock et al. designed molecular receptors with closed-shell cavities containing *in* and/or *out* phosphoryl bridgehead units.[6] However, many of these compounds do not form any complexes with metal ions. Structural constraints and the absence of cooperativity between the binding sites often attenuate the coordinating abilities of the phosphorus units. This article describes a new family of phosphorus ligands in which a phosphorylated binding site is introduced into a semirigid macrocyclic structure. We have recently shown that the synthesis of macrocyclic phosphonamides and the formation of metal ion com-

⊗ Abstract published in *Advance ACS Abstracts,* November 15, 1996.

(1) Ecole Normale Supérieure de Lyon.

(2) Université Catholique de Louvain.

(3) Cram, D. J. *Angew. Chem., Int. Ed. Engl.* **1986**, *25*, 1039.

(4) (a) Caminade, A.-M.; Majoral, J.-P. *Chem. Rev.* **1994**, *94*, 1183. (b) Mitjaville, J.; Caminade, A.-M.; Daran, J.-C.; Donnadieu, B.; Majoral, J.-P. *J. Am. Chem. Soc.* **1995**, *117*, 1712. (c) Sinyavskaya, E. I. *Sov. J. Coord. Chem. (Engl. Transl.)* **1986**, *12*, 663; *Koord. Khim.* **1986**, *12*, 1155. (d) Tsvetkov, E. N.; Bovin, A. N.; Syundyukova, V. Kh. *Russ. Chem. Rev. (Engl. transl.)* **1988**, *57*, 776; *Usp. Khim.* **1988**, *57***,** 1353. (e) Kabachnik, M. I.; Polikarpov, Y. M. *J. Gen. Chem. USSR (Engl. Transl.)* **1988**, *58*, 1729; *Zh. Obsh. Khim.* **1988**, *58*, 1937. (f) Dutasta, J.-P.; Declercq, J.-P.; Esteban-Calderon, C.; Tinant, B. *J. Am. Chem. Soc.*, **1989**, *111*, 7136. (g) Brandt, K.; Porwolik, I.; Kupka, T.; Olejnik, A.; Shaw, R. A.; Davies, D. B. *J. Org. Chem.* **1995**, *60*, 7433. (h) Izatt, R. M.; Lindh, G. C.; Huszthy, P.; Clark, G. A.; Bruening, R. L.; Bradshaw, J. S.; Christensen, J. J. *J. Inclusion Phenom.* **1989**, *7*, 501. (i) Lippmann, T.; Dalcanale, E.; Mann, G. *Tetrahedron Lett.* **1994**, *35*, 1685. (j) Delangle, P.; Dutasta, J.-P. *Tetrahedron Lett.* **1995**, *36*, 9325. (k) Izatt, R. D.; Pawlak, K.; Bradshaw, J. S. *Chem. Rev.* **1991**, *91*, 1721. (l) Savage, P. B.; Holmgren, S. K.; Gellman, S. H. *J. Am. Chem. Soc.* **1994**, *116*, 4069. (m) Savage, P. B.; Holmgren, S. K.; Gellman, S. H. *J. Am. Chem. Soc.* **1993**, *115*, 7900.

(5) (a) Mitjaville, J.; Caminade, A.-M.; Majoral, J.-P. *J. Chem. Soc., Chem. Commun.* **1994**, 2161. (b) Mitjaville, J.; Caminade, A.-M.; Mathieu, R.; Majoral, J.-P. *J. Am. Chem. Soc.* **1994**, *116*, 5007.

(6) (a) Friedrichsen, B. P.; Powell, D. R.; Whitlock, H. W. *J. Am. Chem. Soc.* **1990**, *112*, 8931. (b) Friedrichsen, B. P.; Powell, D. R.; Whitlock, H. W. *J. Am. Chem. Soc.* **1989**, *111*, 9132.

(7) (a) Dutasta, J.-P.; Van Oostenryck, L.; Tinant, B.; Declercq, J.-P. *Phosphorus, Sulfur Silicon Relat. Elem.* **1993**, *75*, 63. (b) Dutasta, J.-P.; Simon, P. *Tetrahedron Lett.* **1987**, *28*, 3577.

S0022-3263(96)01206-6 CCC: $12.00

plexes is possible through the combination of a crown ether unit and a phosphonamide-containing building block.[7−9]

The standard strategy for the synthesis of macrocyclic phosphonamides is the preparation of an intermediate diamine followed by the cyclization of this diamine with a diaminophosphane, and finally oxidation of the parent phosphorus(III) macrocycle.[8,9] This general approach can be applied to a variety of diamines and diaminophosphanes, and syntheses of 17−27-membered-ring phosphorus crown compounds have been developed.[10] In the present study we report the synthesis of the new semirigid macrocyclic ligands **1**−**5** which incorporate the bis(*N*-phenylamino)phosphine oxide or sulfide unit. The 18- and 21-membered macrocycles so produced contain a flexible crown ether part and a rigidified phosphoryl binding unit incorporated into the macrocyclic structure. The complexation of these ligands with alkali metal and ammonium cations as guests has been studied in solution. A detailed investigation of their conformation in solution as well as in the solid state is reported.

Results and Discussion

Synthesis. The synthesis of the macrocyclic phosphonamides **1**−**5** was carried out as reported in Scheme 1 from the macrocyclic precursors **6**−**9**. The rigidification of the corands **6**−**9** was performed by bridging the two amido groups by means of a propyl (**1**−**4**) or ethyl unit (**5**). Corands **6**−**9** were prepared as previously described from the reaction of the apropriate diamine with bis(dimethylamino)methylphosphine followed by the in situ oxidation of the parent P(III) derivative.[8] The rigidification step was carried out using procedures similar to those described by Cram et al. for the synthesis of cyclic urea hemispherand derivatives.[11] The reaction of 1,3-propanediol ditosylate with the macrocycles **6** and **7** in a phase transfer reaction in the presence of aqueous NaOH in biphasic toluene solution results in the formation of the semirigid thiophosphorylated ligands **1** (57%) and **2** (48%). Similarly, ligand **5** was prepared from **9** in biphasic 1,2-dichloroethane in 63% yield. Due to the low solubility of the phosphorylated derivatives **8** and **9** in toluene, these compounds were bridged with 1,3-propanediol ditosylate in the presence of NaH in tetrahydrofuran (THF) to produce **3** (68%) and **4** (78%). Structures of all new compounds were verified by nuclear magnetic resonance (^{1}H, ^{13}C, and ^{31}P NMR), mass spectrometry, and elemental analysis. In addition, crystal structures of three of these new phosphonamide ligands and two of their complexes are provided.

Conformational Analysis of 1−4. The bicyclic structure of the macrocycles **1**−**5** induces conformational rigidity that profoundly influences the structural properties of these ring systems. These conformational changes gain special importance when their relation to the complexing activity of the ligands is considered. When ethyl or propyl bridges are attached to the phosphonamide group of macrocycles **6**−**9**, the resulting five- or six-membered ring introduces conformational restriction which can favor the orientation of the P=O or the P=S bond toward the center of the macrocyclic cavity.

Scheme 1

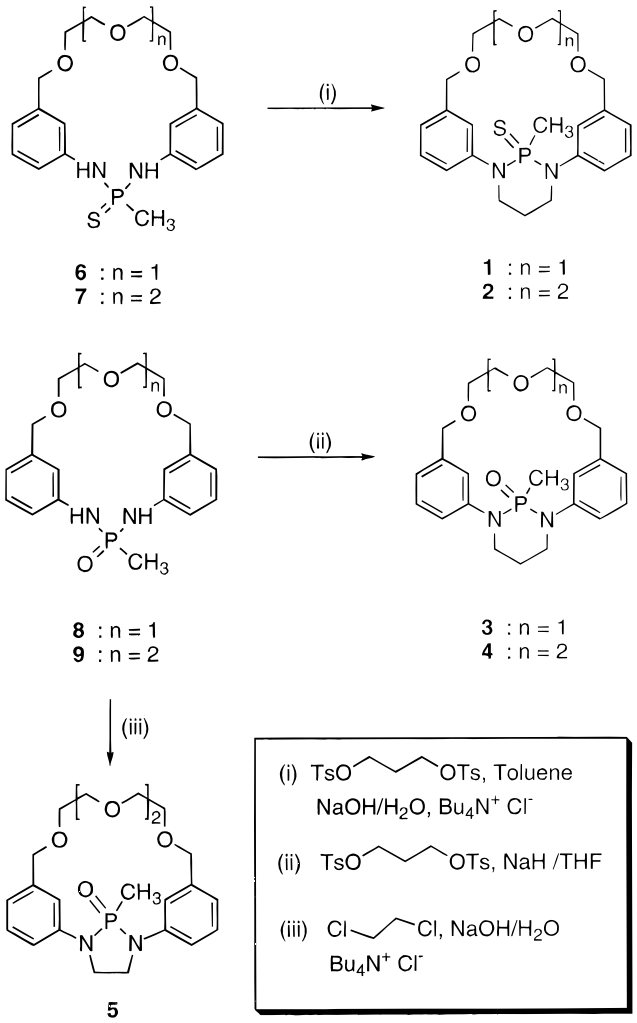

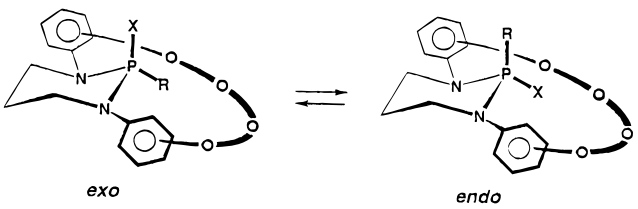

For **1**−**4**, two distinct conformations of the bicyclic molecules are expected which arise from the different *exo* and *endo* orientations of the phosphorus substituents. The *exo* and *endo* forms are related to the outward or inward orientation of the (thio)phosphorylated bond relative to the macrocyclic cavity. Depending on structural considerations and other steric interactions, different degrees of conformational mobility can be found in these macrocycles. Additional conformations are manifested in the solid and liquid phases and arise essentially from the polyether chain. To investigate the degree of preorganization of the binding sites of the macrocyclic phosphonamides, we undertook systematic conformational studies in solution using ^{1}H, ^{13}C, and ^{31}P NMR spectra aided by 2D (COSY, NOESY) and NOE difference experiments.

(8) Van Oostenryck, L.; Tinant, B.; Declercq, J.-P.; Dutasta, J.-P.; Simon, P. *J. Inclusion Phenom.* **1993**, *16*, 383.
(9) Van Oostenryck, L.; Tinant, B.; Declercq, J.-P.; Dutasta, J.-P. *Acta Crystallogr.* **1995**, *C51*, 80.
(10) See refs 7−9 and: Delangle, P.; Van Oostenryck, L.; Declercq, J.-P.; Tinant, B.; Dutasta, J.-P., unpublished work.
(11) (a) Cram, D. J.; Dicker, I. B.; Lauer, M.; Knobler, C. B.; Trueblood, K. N. *J. Am. Chem. Soc.* **1984**, *106*, 7150. (b) Doxsee, K. M.; Feigel, M.; Stewart, K. D.; Canary, J. W.; Knobler, C. B.; Cram, D. J. *J. Am. Chem. Soc.* **1987**, *109*, 3098.

Table 1. *exo/endo* Conformers Ratio of 1 vs Solvent Polarity,[a] and ^{31}P NMR Chemical Shifts (ppm)

solvent	E_T^N	*exo/endo*	δ^{31}P *exo*; *endo*
$CDCl_3$[b]	0.259	75/25	78.3; 69.5
$C_2D_2Cl_4$[c]	0.269	66/34	78.9; 70.3
CD_2Cl_2[c]	0.309	50/50	79.2; 70.6
CD_3COCD_3[b]	0.355	40/60	78.5; 70.2

[a] Determined from the ^{31}P NMR spectra. [b] 27 °C. [c] 33 °C.

The ^{31}P NMR spectrum of **1** at room temperature revealed the presence of two exchangeable signals due to the expected *exo* and *endo* conformers with intensity ratios depending of the solvent polarity. Table 1 gives the different conformer ratios for different solvents whose polarity is expressed through the E_T^N factor.[12] In $CDCl_3$, a 3:1 ratio of the two conformers was observed in favor of the low-field signal. In CD_2Cl_2, a 1:1 ratio was observed, and the proportions were even reversed in acetone to give a 2:3 ratio in favor of the high-field signal. In the ^{31}P spectrum, the coalescence of the signals was observed at high temperature. In $C_2D_2Cl_4$ solution, the two resonances coalesced at 75 °C to give a broad signal which sharpened at higher temperature (75.1 ppm at 120 °C).

The broad signals observed in both the room-temperature ^{1}H and ^{13}C NMR spectra confirm the presence of several conformations interconverting slowly on the NMR time scale. In the low-temperature ^{1}H (8 °C) and ^{13}C (−20 °C) spectra in $CDCl_3$, there is clear evidence for the presence of the two conformers. Interpretation of the 500 MHz ^{1}H−^{1}H g-COSY spectrum of **1** at 10 °C revealed the proton connectivities of the two conformers present in solution in slow exchange conditions on the NMR time scale (Figure 1, Table 2). The low-field aromatic signals at δ 7.74 and 7.86 were unambiguously assigned to the aromatic H(1) protons of the two conformers. The conformational exchange was observed using the NOESY 2D correlation experiment, where NOE interactions were detected between the PCH_3 and the H(1) aromatic protons (Figure 2).

From the examination of molecular models, in the conformer **1**-*exo*, with the methyl group oriented toward the macrocylic cavity, the close proximity of the PCH_3 and the H(1) aromatic protons should allow for an efficient NOE between the two corresponding resonances. The assignment of the two structures was indeed established unambiguously on the basis of 500 MHz NOE difference experiments performed on **1** at −40 °C in $CDCl_3$. The enhancement factor η ($\eta\% = 100(I - I_0)/I_0$) is defined as the NOE at H(1) while saturating the methyl resonance. Irradiation of the 1.62 ppm CH_3 signal caused a strong enhancement of the 7.74 ppm H(1) resonance (η = 5%), while no detectable NOE is observed when irradiating the low-field CH_3 signal (η = 0%). This allowed the assignment of the high-field ^{31}P resonance to the minor *endo* conformation and the low-field signal to the predominant *exo* form.

In the case of the 18-membered P(O) macrocycle **3**, the variable-temperature ^{31}P NMR spectra are consistent with the presence of two conformations exchanging rapidly at room temperature. At 27 °C, only one averaged signal is observed. At temperatures below −20 °C, the two resonances are detected with intensity ratios depending on the solvent. At −50 °C in $CDCl_3$ solution the ^{31}P spectrum exhibits two signals at δ 27.6 (72%) and 33.3 (28%). In CD_2Cl_2 at the same temperature, only one major conformation is observed at δ 27.1.

The ^{1}H resonances of the two conformers were assigned from the 500 MHz COSY-ps 2D correlation experiment, performed at −60 °C in $CDCl_3$ solution (Table 2). NOE measurements were not possible under these conditions because of the fast exchange process at −60 °C. However, with the major conformer at 10 °C in CD_2Cl_2, NOE difference experiments on the PCH_3 and H(1) resonances gave an enhancement factor of 0.8%, a value that allowed the assignment of the low-field signal to the *endo* form of **3**. The conformational equilibrium hinders an unequivocal assignment of the ^{13}C signals for the two conformations in $CDCl_3$. The limiting freezing temperature of the solvent and the fast exchange condition at low temperature prevented the acquisition of a fully interpretable carbon spectra of **3**. Therefore, resonances of the major *endo* conformer were obtained from CD_2Cl_2 solution of **3** at −73 °C (see Experimental Section). However, the time-averaged values $\delta^{13}CH_3$ (10.17 ppm) and $^1J_{PC}$ (115.3 Hz), measured at room temperature in $CDCl_3$, indicate larger values of these parameters for the *exo* conformer following the trend observed for **1**.[13]

Although only limited information is available concerning the solution conformation of 1,3,2-diazaphosphorinanes,[14] the limited number of solid state structures emphasize a predominance of the chair conformation of the six-membered ring.[15,16] In the chair conformation of the closely related six-membered ring 1,3,2-dioxa and 1,3,2-oxazaphosphorinanes, a high-field ^{31}P NMR chemical shift is generally associated with the equatorial orientation of the P=X bond (X = O, S, Se). Moreover, in these systems containing an alkyl or aromatic substituent attached to phosphorus, the value of the $^1J_{PC}$ coupling constant is very sensitive to the conformation around the phosphorus atom and has been widely used as a conformational probe. The largest $|^1J_{PC}|$ value is observed for the equatorial orientation of the P−C bond, $|^1J_{PC}|_{eq} > |^1J_{PC}|_{ax}$.[17] The present observation of the NMR spectra of **1** and **3** at low temperature clearly allows the assignment of the *endo* and *exo* conformations. Thus, the high-field ^{31}P signal associated with smaller values of the $^{13}CH_3$ chemical shift and the $^1J_{PC}$ coupling constant of

(12) Reichardt, C. *Solvents and Solvent Effects in Organic Chemistry*; VCH: Weinheim, Germany, 1990.

(13) One may readily estimate the carbon chemical shift and the $^1J_{PC}$ coupling constant values of the P$^{13}CH_3$ moiety of the *exo* conformer from the time-averaged values measured at room temperature in $CDCl_3$. Thus: $^1J_{PC}$(obsd) = N(**3-*exo***)$^1J_{PC}$(**3-exo**) + N(**3-*endo***)$^1J_{PC}$(**3-*endo***) where N is the mole fraction of **3-*exo*** or **3-*endo*** determined from the ^{31}P NMR spectrum at −50 °C. Therefore, $^1J_{PC}$(**3-*exo***) = [1/N(**3-*exo***)][$^1J_{PC}$(obsd) − N(**3-*endo***)$^1J_{PC}$(**3-*endo***)] = 121 Hz. A similar derivation involving $\delta^{13}CH_3$(obsd) gives a completely analogous equation to estimate δ $^{13}CH_3$(**3-*exo***) = 16 ppm.

(14) Maryanoff, B. E.; Hutchins, R. O.; Maryanoff, C. A. *Top. Stereochem.* **1979**, *11*, 187.

(15) (a) Denmark, S. E.; Swiss, K. A.; Wilson, S. R. *J. Am. Chem. Soc.* **1993**, *115*, 3826. (b) Dutasta, J.-P.; Esteban-Calderon, C.; Tinant, B.; Declercq, J.-P. *Acta Crystallogr.* **1990**, *C46*, 68. (c) Engelhardt, U.; Scheffler, B. *Acta Crystallogr.* **1989**, *C45*, 775.

(16) (a) Denmark, S. E.; Miller, P. C.; Wilson, S. R. *J. Am. Chem. Soc.* **1991**, *113*, 1468. (b) Denmark, S. E.; Dorow, R. L. *J. Am. Chem. Soc.* **1990**, *112*, 864.

(17) (a) Denmark, S. E.; Chen, C.-T. *J. Am. Chem. Soc.* **1995**, *117*, 11879. (b) Bentrude, W. G.; Setzer, W. N.; Sopchik, A. E.; Chandrasekaran, S.; Ashby, M. T. *J. Am. Chem. Soc.* **1988**, *110*, 7119. (c) Bentrude, W. G.; Sopchik, A. E.; Bajwa, G. S.; Setzer, W. N. *Acta Crystallogr.* **1986**, *C42*, 1027. (d) Bentrude, W. G.; Sopchik, A. E.; Setzer, W. N.; Bates, R. B.; Ortega, R.B. *Acta Crystallogr.* **1986**, *C42*, 584. (e) Stec, W. J.; Zielinski, W. S. *Tetrahedron Lett.* **1980**, *21*, 1361. (f) White, D. W.; Gibbs, D. E.; Verkade, J. G. *J. Am. Chem. Soc.* **1979**, *101*, 1937. (g) Lesiak, K.; Uznanski, B.; Stec, W. J. *Phosphorus* **1975**, *6*, 65. (h) Stec, W. J.; Lesiak, K.; Mielczarek, D.; Stec, B. *Z. Naturforsch.* **1975**, *30b*, 710.

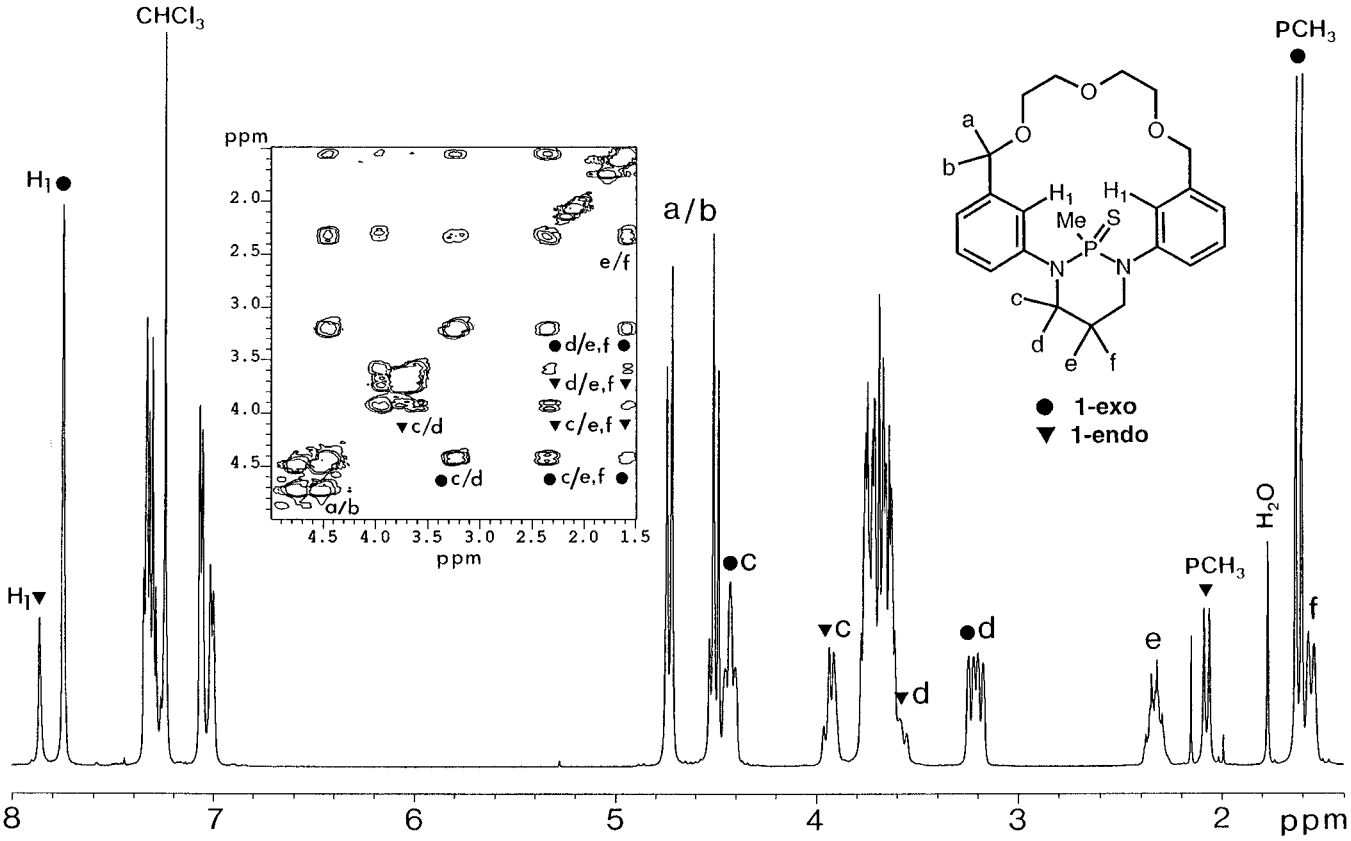

Figure 1. ^{1}H NMR (500 MHz, $CDCl_3$) spectrum of **1**. The inset shows the ^{1}H−^{1}H chemical shift correlation map (g-COSY) of the methyl and methylene region.

Table 2. Selected ^{31}P, ^{1}H, and ^{13}C NMR Chemical Shifts (ppm), and Proton−Phosphorus and Carbon−Phosphorus Coupling Constants (Hz) for Compounds 1−4

	1			**3**		
conformation	*exo*	*endo*	**2** *exo*	*exo*	*endo*	**4**
δ^{31}P in $CDCl_3$	78.64	70.38	81.22	33.29	27.61	25.22
(temp, °C)	(−40)	(−40)	(27)	(−50)	(−50)	(27)
δ^1H[a]						
H(1)	7.74	7.86	7.46	7.70	7.91	7.76
NCH_2	4.43	3.90	4.03	4.21	3.82	3.65
	3.21	3.60	3.26	3.30	3.82	3.65
CH_2	2.33	2.33	2.23	2.33	2.15	2.35
	1.56	1.56	1.93	1.58	1.58	2.02
PCH_3	1.62	2.05	1.76	1.34	1.61	1.32
($^2J_{PH}$)	(14.1)	(12.8)	(13.5)	(14.9)	(14.3)	(14.6)
$\delta^{13}C(PCH_3)$[b]	20.57	16.09	22.02		7.89	10.59
($^1J_{PC}$)	(92.8)	(86.8)	(93.7)		(113.2)	(114.8)

[a] 500 MHz in $CDCl_3$; 8 (**1**), 20 (**2**), −60 (**3**), and 10 °C (**4**). [b] $CDCl_3$, −20 (**1**), and 27 (**2**, **4**); CD_2Cl_2, −73 °C (**3**).

the *endo* form indicate a dominant chair conformation with an axially oriented PCH_3 substituent. Similar conclusions arise for the *exo* conformation, which exhibited low-field ^{31}P resonance associated to larger $\delta^{13}CH_3$ and $^1J_{PC}$ values (Table 2).

These results are consistent with the equilibrium involving *exo* and *endo* forms of **1** and **3**, presumably by inversion of the diazaphosphorinane heterocycle, concomitantly with bond rearrangements around the nitrogen atoms. As viewed from the X-ray crystallographic structures described in the next section, the rather trigonal-planar ring nitrogen atoms lead to aromatic rings having no marked axial or equatorial orientations, suggesting that such a bond rearrangement is of low cost in energy compared to ring flipping. This process does not need the passage of the whole six-membered ring through the annulus of the macrocycle, which is probably a higher energy process. In its chair conformation, the inversion of the six-membered heterocycle exchanges the axial and equatorial positions of the phosphorus substituents leading to the *exo* and *endo* conformations of the ligands. Simulation of the dynamic behavior of the ^{31}P NMR spectra of **1** and **3** by line shape analysis at different temperatures allowed the determination of the free energy of the barrier of the ring flipping.[18] The bulky P(S) group yields a higher energy barrier of interconversion relative to the smaller P(O) group ($\Delta G^*_{endo\rightarrow exo} = 16.0$ and 11.9 kcal/mol, respectively).

The 21-membered rings **2** and **4** have also been investigated. No evidence for chemical exchange was detected by NMR for these compounds even at low temperature. However, a certain analogy seems to emerge with the NMR data of compounds **1**−**4**. According to the values of the ^{31}P and ^{13}C NMR data of **1** and **2** reported in Table 2, it is tempting to assign the *exo* conformation to the conformer of **2** observed in $CDCl_3$ at room temperature. Indeed, **1-*exo*** and **2** exhibit similar δ^{31}P and $\delta^{13}C(PCH_3)$ chemical shifts and $^1J_{PC}$ coupling constants. Furthermore, the NOE difference experiment performed with **2** at 10 °C gave an important NOE response ($\eta = 10\%$). This finding reinforces the conclusion that macrocycle **2** mainly exists as the *exo* conformation, which is the conformation observed in the solid state (see below).

The situation observed for **4** is somewhat different. From the NMR data reported in Table 2 and particularly the NOE measured at 10 °C in $CDCl_3$ ($\eta = 2.5\%$), the conformational behavior of **4** can be interpreted in terms

(18) Martin, M. L.; Martin, G. J.; Delpuech, J.-J. *Practical NMR Spectroscopy*; Heyden: Chichester, England, 1980; p 291.

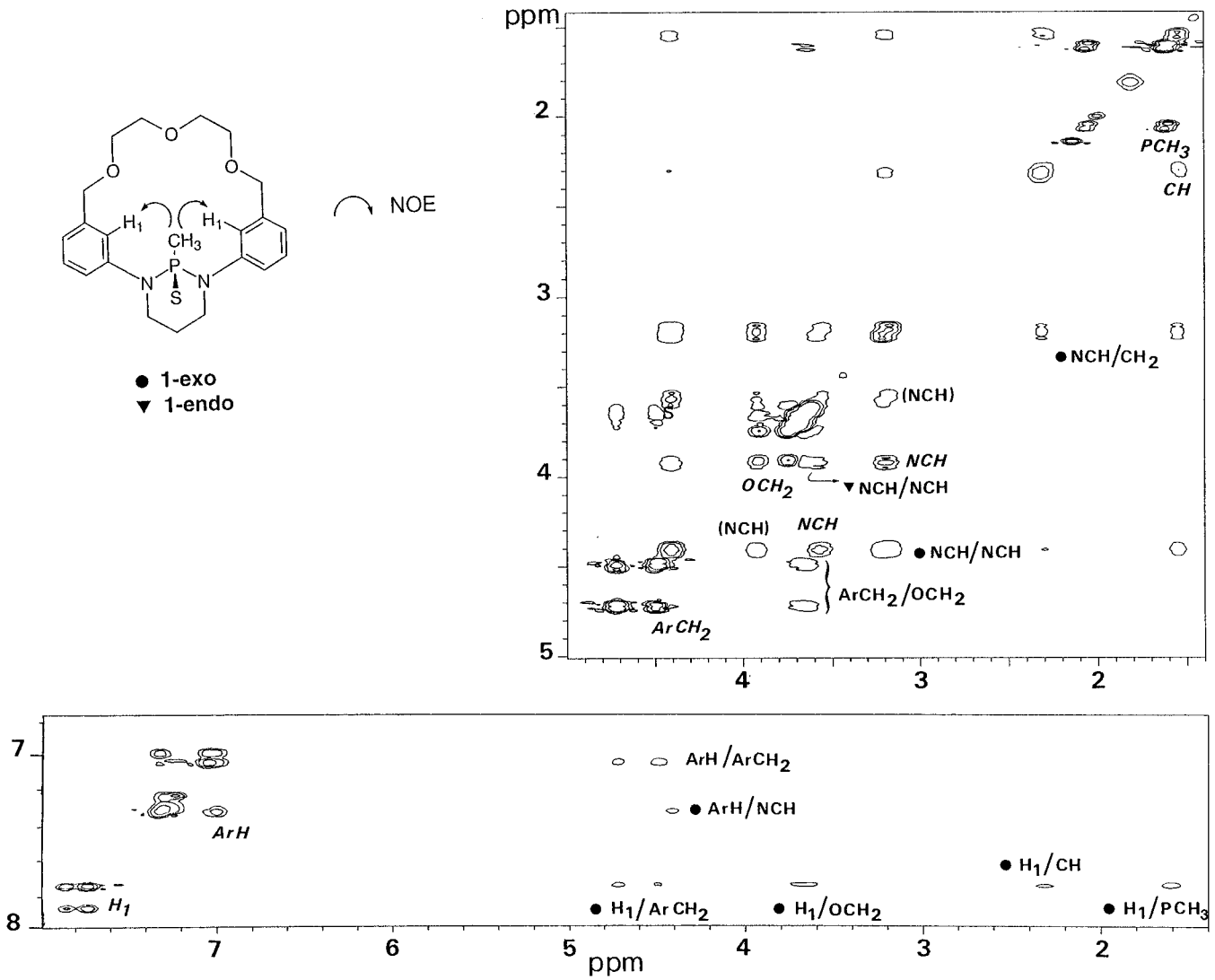

Figure 2. Sections of 500 MHz NOESY spectrum of **1** in $CDCl_3$ at 2 °C: (top) methyl and methylene region; (bottom) aromatic region. Exchange cross-peaks are in italic; cross peaks in parentheses are due to relayed NOE.

of (i) a single predominant conformation in solution or (ii) a rapid exchange between two unequally populated conformations which are still rapidly exchanging at −90 °C. We will tentatively interpret the above data in terms of the equilibrium between a minor *exo* form and a predominant *endo* conformation. This is supported by the high-field ^{31}P and $^{13}CH_3$ chemical shifts, the $^1J_{PC}$ coupling constant value, and the moderate NOE. Nonetheless, we should keep in mind the possibility of other nonchair conformations of the diazaphosphorinane ring, which could contribute to the interconversion pathway.

X-ray Crystallographic Analysis. Among the attempted recrystallization of hosts **1**−**5**, only those described below afforded crystals of X-ray quality. Therefore, the solid state structures of **1**, **2**, and **5** were determined to assess the degree of structural preorganization of the ligand prior to complexation. As examined above, two different conformations are expected for the bicyclic structures which were characterized as the *exo* and *endo* forms due to the different orientations of the phosphoryl or thiophosphoryl moieties. Complex formation will be fundamentally dependent on the conformation of the ligand, and only the *endo* form is able to form stable intracavity complexes with coordination to the phosphoryl moiety. The complexing properties of the phosphorylated **3**−**5** were investigated with respect to the hard alkali metal and ammonium cations (see below). It is well-known that sulfur acts as an efficient donor atom for soft metal ions. Thus, on replacing the P(O) donor goup with the thiophosphoryl P(S) group, the affinity of the ligands toward alkali metal cations should decrease while affinity toward soft metals should increase. We further tested the complexing capability of the thiophosphorylated ligand **1** for soft metal cations such as Hg^{II}. Interestingly, single crystals of the complexes **1**·$Hg(SCN)_2$ and **5**·$LiNO_3$ appropriate for X-ray analysis were obtained, and a comparison of their solid state structures with that of the free ligands was possible.

The 18-membered ring **1**, which exists in solution as a mixture of *exo* and *endo* conformers, crystallized as the *endo* form (Figure 3). In the asymmetric conformation of **1** observed in the solid state, the diazaphosphorinane ring adopts a chair conformation with the sulfur atom in the equatorial position so that the P═S bond turns inward the macrocyclic cavity. The $(ag^+g^-)(ag^-a)$ arrangement of the diethyleneoxy chain introduces a pseudocorner, and consequently the O(11) atom is directed outward. As indicated by the sum of the two N-atom bond angles (348.8 and 351.7°), the nonplanarity of the nitrogen atoms forces the two aromatic rings to adopt two different orientations, pseudoaxial and pseudoequatorial, introducing the asymmetry of the whole

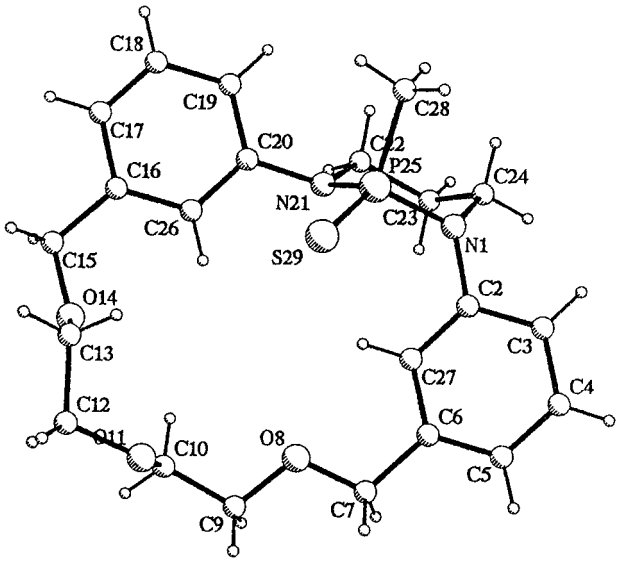

Figure 3. Molecular structure of **1**.[32]

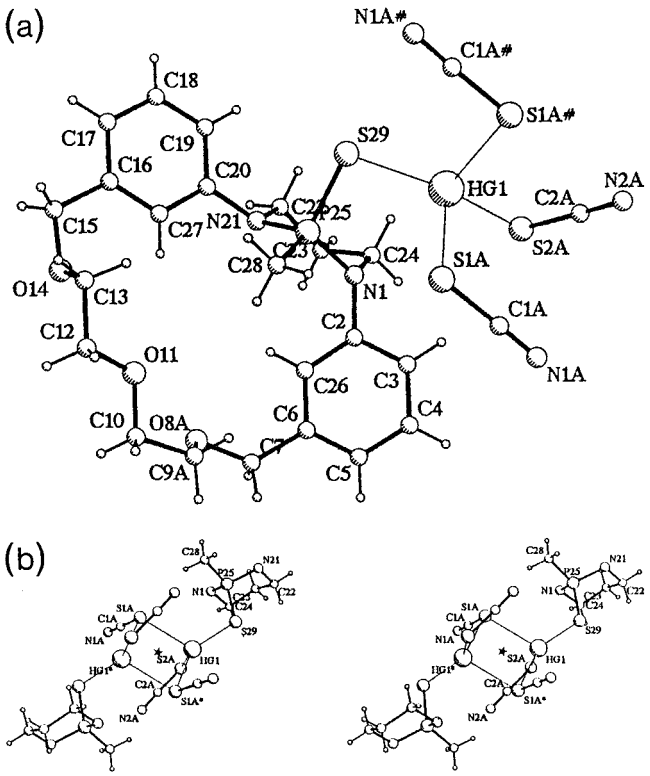

Figure 4. Molecular structure of **1**·$Hg(SCN)_2$ (a) and part of the stereoscopic view showing the dimeric arrangement in the complex (b).[32]

macroring as viewed on Figure 3. In this structure, the benzene rings are almost orthogonal to the C−N−P plane of the six-membered ring (dihedral angles are 77 and 81°). The well-defined macrocyclic cavity is partly occupied by the two aromatic protons C(26)H and C(27)H and the C(10)H_2 and C(13)H_2 groups of the polyether chain.

In the mercury complex **1**·$Hg(SCN)_2$, the most striking observation is the exocyclic coordination of the Hg^{2+} cation by the P(S) donor group. The *exo* orientation of the P═S bond has only little effect on the conformation of the host molecule (Figure 4). The six-membered heterocycle still adopts a chair conformation with the P═S group axial and the P−CH_3 group equatorial and

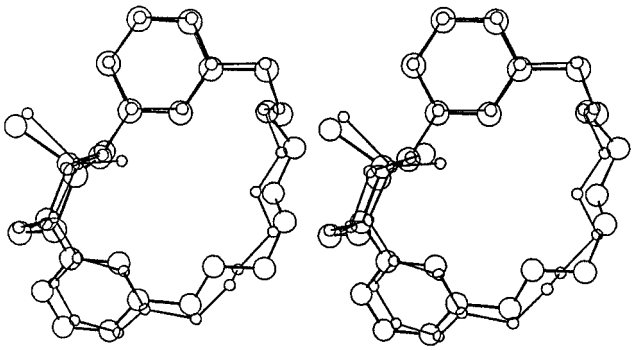

Figure 5. Superposition of the conformations of the macrocycle in **1** and in the complex **1**·$Hg(SCN)_2$.[33]

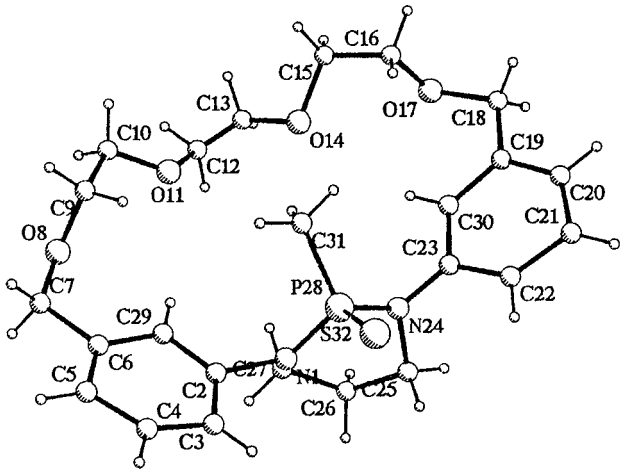

Figure 6. Molecular structure of **2**.[32]

directed toward the macrocyclic cavity. The torsional angles of the diazaphosphorinane rings are comparable in **1** (49.4, −44.6, 49.9, −55.5, 60.9, −60.9°) and **1**·$Hg(SCN)_2$ (50.9, −47.6, 53.9, −60.5, 62.6, −59.2°). Although a disorder of the O(8)−C(9) bond is observed in **1**·$Hg(SCN)_2$, the whole macrocyclic structure adopts a conformation very similar to that observed with the free ligand **1** as viewed on Figure 5. The complex forms dimers where the two molecules are bound through the sulfur atoms of the thiocyanate anions (Figure 4). The Hg^{2+} ion is best described as the center of a distorted terahedral array of four S donor atoms. Three S atoms of the thiocyanate anions (Hg···S(1A) = 2.823(2) Å; Hg···S(2A) = 2.437(2) Å; Hg···S(1A)* = 2.626(2) Å) and the thiophosphoryl S donor atom (Hg···S(29)P = 2.417(1) Å) are coordinated (S(1A)* is related by a center of symmetry to S(1A)). The intermolecular Hg···Hg distance is 3.879(1) Å. The coordination of only the P(S) donor group of the ligand to Hg with no participation of any oxygen ether donors was not unexpected because of the thiophilic character of the soft Hg^{2+} cation.

Interestingly, the 21-membered ring **2** adopts the *exo* conformation with the P═S bond oriented away from the macrocyclic cavity (Figure 6). The $(ag^-a)(g^+g^+a)(ag^+a)$ conformation of the polyether chain of the molecule is rather unusual with two adjacent gauche bonds of the same sign (C(10)−O(11)−C(12)−C(13) = 116°, O(11)−C(12)−C(13)−O(14) = 41°), which however does not affect dramatically the favorable orientation of the oxygen atoms toward the center of the macroring. The macrocyclic cavity is occupied by the aromatic hydrogen atoms C(29)H and C(30)H and the methyl group bound to the phosphorus atom. The diazaphosphorinane ring adopts

Table 3. Selected Bond Lengths and Bond Angles around the Phosphorus Atom in 1, 1·Hg(SCN)$_2$, 2, 5, and 5·LiNO$_3$

	distances (Å) and angles (deg)				
	1	**1**·Hg(SCN)$_2$	**2**	**5a** **5b**	**5**·LiNO$_3$
P═S(O)	1.929(1)	2.019(2)	1.934(2)	1.468(3) 1.459(3)	1.478(3)
P—C	1.798(3)	1.774(5)	1.793(6)	1.774(5) 1.783(5)	1.805(4)
P—N(*x*)	1.685(2)	1.663(4)	1.708(10)	1.678(3) 1.670(4)	1.658(2)
P—N(*y*)	1.659(2)	1.642(4)	1.610(10)	1.669(4) 1.670(4)	1.658(2)
C—P═S(O)	111.2(1)	110.7(2)	110.7(2)	112.6(2) 107.6(2)	110.5(2)
N(*x*)—P—N(*y*)	103.2(1)	106.4(2)	98.5(3)	93.6(2) 93.0(2)	95.0(2)
(O)S═P—N(*x*)	113.1(1)	109.3(2)	115.4(4)	114.8(2) 117.6(3)	116.6(1)
(O)S═P—N(*y*)	116.0(1)	110.1(2)	115.7(4)	117.8(2) 116.6(2)	116.6(1)
C—P—N(*x*)	108.9(1)	109.8(2)	107.5(6)	109.0(2) 108.2(2)	108.5(1)
C—P—N(*y*)	103.7(1)	110.5(2)	108.1(5)	107.4(2) 107.6(2)	108.5(1)
P—N(*x*)—C	117.2(2)	113.0(3)	115.3(7)	111.8(3) 113.4(3)	112.8(2)
P—N(*y*)—C	114.8(2)	113.5(3)	123.3(8)	111.3(3) 111.9(3)	112.8(2)
P—N(*x*)—C$_{aro}$	117.5(2)	117.6(3)	117.6(8)	123.1(3) 125.0(3)	127.1(2)
P—N(*y*)—C$_{aro}$	122.3(2)	123.0(3)	118.6(7)	125.9(3) 121.2(3)	127.1(2)
C—N(*x*)—C$_{aro}$	114.1(2)	114.4(4)	119.7(9)	118.7(4) 120.3(4)	120.0(2)
C—N(*y*)—C$_{aro}$	114.6(2)	115.9(4)	112.7(10)	122.5(3) 120.4(4)	120.0(2)

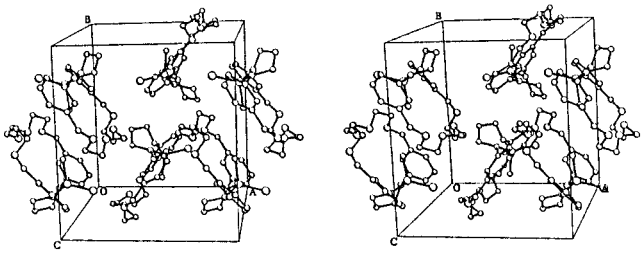

Figure 7. Stereoview of the molecular packing in the unit cell of **2**.[32]

a twist boat (TB) conformation,[19] a pseudotwofold axis passing through the midpoints of the N(1)—C(27) and N(24)—C(25) bonds. The nitrogen atoms are slightly pyramidal as their bond angles summed are 352.6 and 354.6° (Table 3). No specific interaction is involved in the packing of the molecules in the unit cell (Figure 7). The macrorings face each other in a head to tail arrangement.

In **5** two different molecules, **5a** and **5b**, exist in the crystal. The molecules are practically mirror images of each other with different conformations arising from the polyethylene chain and a slightly different conformation of the diazaphospholane ring (half-chair in **5a** (endocyclic torsion angles 16, 8, −28, 37, and −34°, $\Delta C_2 = 7.1°$) and envelope in **5b** (endocyclic torsion angles −16, −5, 23, −33 and 32°, $\Delta C_s = 7.1°$)).[20] In contrast to **2**, the two aromatic rings are nearly coplanar with the mean plane of the diazaphospholane heterocycle, with tilting angles of 14 and 26° in **5a**, 27 and 10° in **5b**. Owing to the rigid geometry of the 1,3-diphenyl-1,3,2-diazaphospholane segment, the 21-membered macrocycle is more strained and defines an extended ovoid cavity with isoclinal P═O and P—CH$_3$ bonds oriented inward (Figure 8).

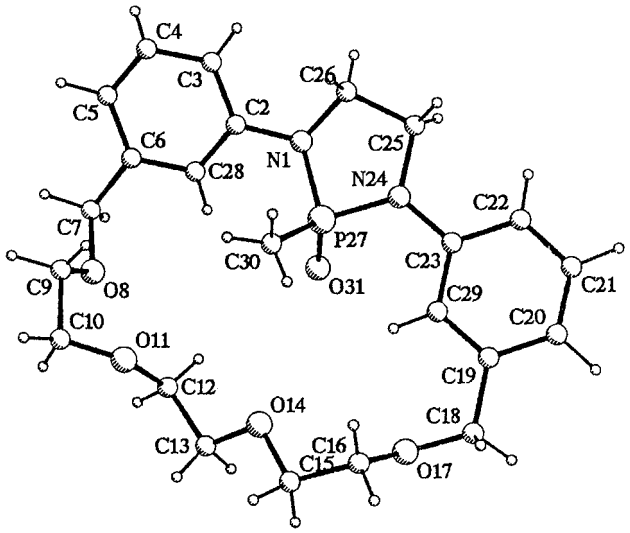

Figure 8. Molecular structure of one of the two independent molecules of **5** (**5b**).[32]

The conformations adopted by both **5** and its Li$^+$ complex are basically similar. The polyether chain of the complex adopts a conformation slightly different from that of the free ligand, favoring the metal ion coordination. In the structure of **5**·LiNO$_3$, the Li$^+$ cation is bound

(19) Hendrickson, J. B. *J. Am. Chem. Soc.* **1964**, *86*, 4854.

(20) (a) Duax, W. L.; Weeks, C. M.; Rohrer, D. C. *Top. Stereochem.* **1976**, *9*, 271. (b) Hargis, J. H.; Jennings, W. B.; Worley, S. D.; Tolley, M. S. *J. Am. Chem. Soc.* **1980**, *102*, 13. (c) Koeller, K. J.; Rath, N. P.; Spilling, C. D. *Acta Crystallogr.* **1993**, *C49*, 1199. (d) Bélanger-Gariépy, F.; Delorme, D.; Hanessian, S.; Brisse, F. *Acta Crystallogr.* **1986**, *C42*, 856. (e) Light, R. W.; Campana, C. F.; Paine, R. T. Morosin, B. *Acta Crystallogr.* **1978**, *B34*, 3671.

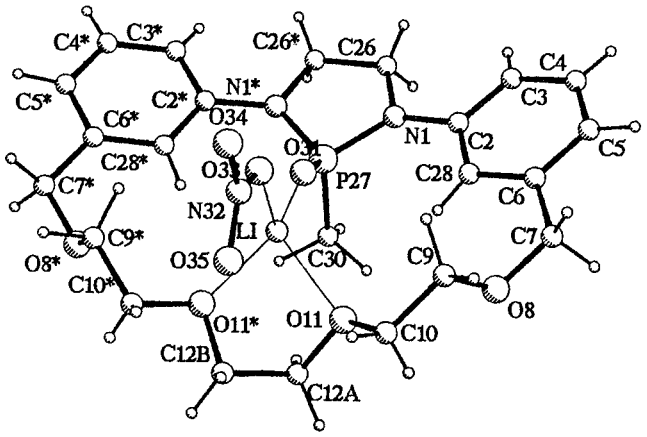

Figure 9. Molecular structure of the complex **5**·$LiNO_3$.[32]

to four atoms: two symmetry-related atoms of the four crown O atoms, the phosphoryl O atom, and one oxygen atom of the nitro group, which together approximately yield a tetrahedral array (Figure 9). Oxygen atoms O(8) and O(8)* fail to coordinate, apparently because of the increased strain of the macrocyclic structure imposed by the five-membered heterocycle. Lithium−oxygen bonds yield short distances (1.878(7), 2.038(5), 2.038(5), 1.918(7) Å) with the shortest distance to the phosphoryl O atom. The Li···ONO_2 distance (1.918(7) Å) compares closely with those in some previously reported Li−$O_3(NO_3)$ complexes.[21] The short 1.878 Å P═O···Li^+ distance supports the strong coordination of the Li^+ cation to the phosphoryl unit.[22] It is even shorter than the P═O···Li^+ distances reported for lithiated phosphonyl compounds (1.912−1.922 Å).[16] The 2.038 Å Li^+···O lengths agree well with the reported values for crown ether oxygen bound to Li^+ with averaged distances of 2.04−2.10 Å.[23]

It is tempting to suggest that the solid state structures of the P(S) derivatives **1** and **2** make reasonable models for the P(O) ligands **3** and **4**, which can adopt similar conformations in the solid state. As we will see for the interpretation of the picrate extraction experiments described below, it should be kept in mind that the *exo* orientation of a P═O bond is unfavorable for the formation of strong complexes. A structural reorganization will thus be needed to afford the best structure allowing the phosphoryl binding unit to coordinate to the cationic guest.

Solution Complexation. The capability of receptors **3**,[24] **4**, and **5** to complex alkali metal and ammonium cations was evaluated by using the picrate extraction method reported by Cram et al.[25] In Table 4, it is shown that the 21-membered ring **4**, which bears five binding sites, forms stronger complexes than **3** and **5** and presents a marked selectivity for K^+ and NH_4^+ cations (-$\Delta G°$ = 7.3 and 8.0 kcal/mol, respectively) (Figure 10). We have shown that in solution the predominent *endo* conformer coexists with another conformation that we tentatively assigned to the *exo* form. Therefore, these relatively low values are attributed to the necessary conformational reorganization of part of the ligand for complexation to occur with participation of the phosphoryl moiety.

The low selectivity observed with the complexes of **3** and **5** reflects that the number of binding sites, the length of the crown ether part of the macrocycle, and the conformation around the phosphorus atom are predominant factors. The smaller macrocycle **3** has only four donor sites, and its cavity is partially occupied by the hydrogen of the aromatic rings. This situation is probably unfavorable to the formation of stable 1:1 complexes. However, the larger ligand **5**, which possesses the same binding sites as **4**, adopts a rather rigid conformation due to the five-membered diazaphospholane ring, which induces more strain throughout the structure of the macrocyclic cavity and tends to give an ovoid planar structure. This situation is clearly demonstrated in the solid state structure of the ligand and its lithium complex (Figures 8 and 9, respectively). In this latter case, no conformational reorganization is possible as the macrocycle adopts a rigid conformation with the phoshoryl group oriented inward. We can conclude for **5** that the low degree of preorganization does not arise from the lack of rigidity but from the topological organization of the host.

Owing to the lack of structural data for **3** and **4**, it is however difficult to ascertain the stabilization effect inferred by the presence of the phosphoryl group in these ligands. Its contribution and the conformational rearrangement can mutually vanish and interfere to a greater or lesser extent with the overall stability constants as determined in the picrate experiments. However, we believe that the stabilization inferred by P═O coordination could be significantly larger. Further studies toward hemispherand like structures are currently in progress to confirm this idea.

Conclusion

Alkylation of the NH functions of the macrocyclic phosphonamides with ethylene or propylene bridges proved to be an efficient route to a new family of semirigid phosphorylated macrorings. ^1H and ^{31}P NMR spectroscopical investigations were used for structural investigations in solution. With the more conformationally restricted macrocycles **1** and **3**, the *exo* and *endo* conformations are both present at room temperature. With the larger ligand **2**, the *exo* conformation dominates, whereas **4** exists as rapidly exchanging conformers. The *exo*−*endo* equilibrium is thus temperature and solvent polarity dependent, and the ring inversion of the diazaphosphorinane moiety in **1** and **3** is a possible process for the conformationnal exchange. As viewed from the solid state molecular structure, **5** adopts a more rigid conformation due to the five-membered diazaphospholane ring. Consequently the P═O bond is oriented toward the macrocyclic cavity in one predominant conformation. NMR data are consistent with this structure.

The stability constants of the complexes reported herein provide significant evidence for the efficient binding properties of the phosphoryl unit for alkali metal and ammonium cations. The complexation of these cations

(21) Raston, C. L.; Whitaker, C. R.; White, A. H. *Aust. J. Chem.* **1988**, *41*, 1917.
(22) Barr, D.; Doyle, M. J.; Mulvey, R. E.; Raithby, P. R.; Reed, D.; Snaith, R.; Wright, D. S. *J. Chem. Soc., Chem. Commun.* **1989**, 3418.
(23) (a) Shoham, G.; Lipscomb, W. N.; Olsher, U. *J. Chem. Soc., Chem. Commun.* **1983**, 208. (b) Delgado, M.; Wolf, R. E.; Hartman, J. R.; McCafferty, G.; Yagbasan, R.; Rawle, S. C.; Watkin, D. J.; Cooper, S. R. *J. Am. Chem. Soc.* **1992**, *114*, 8983.
(24) Values for **3** in Table 4 are more accurate than those previously reported in ref 7a.
(25) (a) Kyba, E. P.; Helgeson, R. C.; Madan, K.; Gokel, G. W.; Tarnowski, T. L.; Moore, S. S.; Cram, D. J. *J. Am. Chem. Soc.* **1977**, *99*, 2564. (b) Koenig, K. E.; Lein, G. M.; Stuckler, P., Kaneda, T.; Cram, D. J. *J. Am. Chem. Soc.* **1979**, *101*, 3553. (c) Helgeson, R. C.; Weisman, G. R.; Toner, J. L.; Tarnowski, T. L.; Chao, Y.; Mayer, J. M.; Cram, D. J. *J. Am. Chem. Soc.* **1979**, *101*, 4928.

Table 4. Association Constants (K_a) and Free Energies of Binding ($-\Delta G°$) of Picrate Salt Guests to Hosts 3−5 in $CHCl_3$ Saturated with H_2O

	3[a]		4[b]		5[b]	
cations	$K_a \times 10^{-3}$ (L/mol)	$-\Delta G°$ (kcal/mol)	$K_a \times 10^{-3}$ (L/mol)	$-\Delta G°$ (kcal/mol)	$K_a \times 10^{-3}$ (L/mol)	$-\Delta G°$ (kcal/mol)
Li^+	4.58	5.01	39.3	6.14	21.2	5.76
Na^+	11.6	5.57	60.0	6.39	16.6	5.63
K^+	12.6	5.61	308	7.34	16.3	5.61
Rb^+	18.3	5.84	192	7.06	17.7	5.67
Cs^+	15.6	5.74	107	6.73	11.1	5.40
NH_4^+	23.5	5.99	980	8.01	11.8	5.44
$CH_3NH_3^+$	19.5	5.87	116	6.77	8.1	5.22
$^tBuNH_3^+$	9.47	5.45	55.9	6.35	3.2	4.68

[a] Measured at 26 °C. [b] Measured at 19 °C.

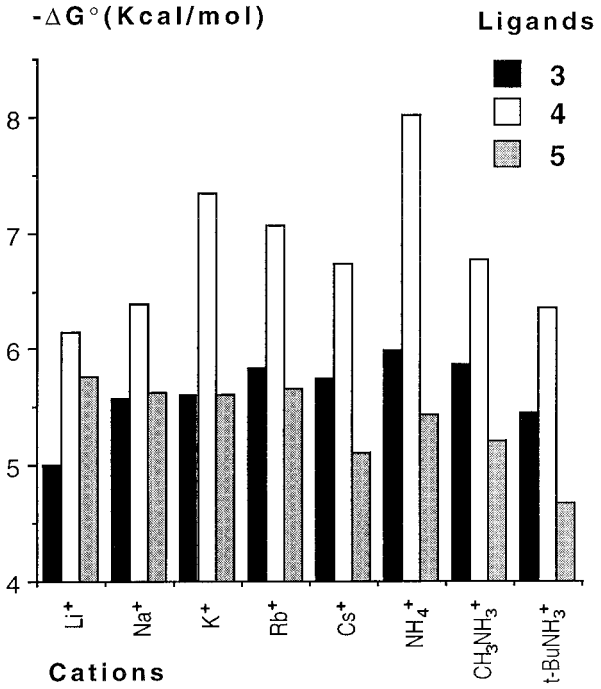

Figure 10. Bar diagram of the free energies of complexation for **3**, **4**, and **5**, as obtained from the picrate extraction experiments.

requires a sufficient degree of preorganization of the ligand. The hosts undergo partial rearrangement during the complexation process as the phosphoryl group has to be directed toward the center of the macrocyclic cavity (*endo* form) to cooperatively coordinate cationic species. The structural studies of the phosphonamide macrocycles **1**, **2**, and **5** and the lithium complex **5**·Li^+, highlight this point. This process is the reason for the relatively low stability constants measured with these derivatives of the crown ether family and demonstrates the importance of the preorganization principle. The P═O bond can be involved in strong hydrogen bonding and favors complex formation with ammonium cations. The mercury complex **1**·Hg^{2+} showed the extra cavity coordination of the metal ion with no participation of the hard donor oxygens of the crown part of the molecule. The Hg^{2+} cation is bound to the P═S unit which is directed away from the macrocyclic cavity of **1**.

Experimental Section

General Information. All manipulations involving air-sensitive species were carried out under dry nitrogen or argon. THF was distilled from Na/benzophenone prior to use. Toluene was distilled from Na. ^1H, ^{13}C, and ^{31}P NMR spectra were recorded on Varian Unity 500 and Bruker AC200 or AM300 spectrometers. Chemical shifts are in δ values from Me_4Si (^1H and ^{13}C) or H_3PO_4 85% (^{31}P). ^{13}C and ^{31}P NMR spectra are proton decoupled unless otherwise noted. The reported multiplicities of ^{13}C NMR spectra represent $^{31}P-^{13}C$ couplings. ^{13}C assignments were mainly based on DEPT spectra. Some of the ^1H and ^{13}C resonances were assigned by means of 2D NMR correlation experiments at low temperature. For each 2D NMR experiment, a total of 256 increments of 1K or 2K data points were collected. g-COSY spectra were recorded in the absolute mode, while COSY and NOESY spectra were recorded in the phase-sensitive mode. NOESY spectra were recorded with relaxation delay $D_1 = 3$ s and mixing time $\tau =$ 500 ms. For NOE difference spectra, separate free induction decays were accumulated for the on-resonance irradiations and the control spectrum with 3 s prescan saturation time. Elemental analyses were performed by the Service Central d'Analyses, CNRS. Melting points are uncorrected. Reactions were monitored by ^{31}P NMR, thin-layer chromatography (Merck Kieselgel 60F254), and analytical size exclusion chromatography (Merck Lichrogel PS, using dichloromethane as the mobile phase). Silica gel used for column chromatography was Merck Kieselgel 60. 1,3-Propanediol ditosylate was prepared as described.[26] Macrocyclic precursors **6**−**9** were synthesized according to a previously described procedure.[8]

25-Methyl-8,11,14-trioxa-1,21,25-diazaphosphatetracyclo[19,3,1,$1^{2,6}$,$1^{16,20}$]heptacosa-2,4,6(26),16,18,20(27)-hexaene 25-Sulfide (1). To a stirred mixture of **6** (500 mg, 1.3 mmol), 1,3-propanediol ditosylate (540 mg, 1.4 mmol), and tetrabutylammonium chloride (100 mg, 0.34 mmol) in toluene (130 mL) was added a solution of NaOH (1.52 g, 38 mmol) in water (15 mL). The resultant mixture was heated to 70 °C and vigorously stirred for 2 days. The reaction mixture was cooled to room temperature, and the water layer was extracted with toluene. The combined toluene extracts were washed with water and brine, dried (MgSO4), filtered, and evaporated under vacuum. Silica gel column chromatography (ethyl acetate/dichloromethane 1:9) of the residue afforded **1** (320 mg, 57%) as a white powder which can be recrystallized from acetone: mp 154 °C; EIMS *m/z* 432 (M^+). Anal. Calcd for $C_{22}H_{29}N_2O_3PS$: C, 61.09; H, 6.76; N, 6.48; P, 7.16; S, 7.41. Found: C, 60.81; H, 6.67; N, 6.34; P, 7.04; S, 7.15.

1-*exo*: ^1H NMR (500 MHz, 281 K, $CDCl_3$) δ 1.56 (m, 1H, CH_2), 1.62 (d, $^2J(P,H) = 14.1$ Hz, 3H, PCH_3), 2.33 (m, 1H, CH_2), 3.21 (m, 2H, NCH_2), 3.55−3.80 (m, 8H, OCH_2), 4.43 (m, 2H, NCH_2), 4.50, 4.74 (d_{AB}, $^2J(A,B) = 12.8$ Hz, 4H, $ArCH_2$), 7.06 (d, $J = 7.0$, 2H, ArH), 7.30 (m, 4H, ArH), 7.74 (s, 2H, ArH); ^{13}C NMR (75 MHz, 253 K, $CDCl_3$) δ 20.6 ($J = 92.8$ Hz, PCH_3), 24.1 (CH_2), 49.7 (NCH_2), 69.3, 70.8, 72.1 (OCH_2), 125.2 ($J =$ 1.7 Hz, ArCH), 126.4 ($J = 3.5$ Hz, ArCH), 126.8 ($J = 5.7$ Hz, ArCH), 129.5 (ArCH), 138.9 ($J = 1.6$ Hz, ArCq), 145.8 ($J =$ 2.9 Hz, ArCq); ^{31}P NMR (81 MHz, 233 K, $CDCl_3$): $\delta = 78.64$.

1-*endo*: ^1H NMR (500 MHz, 281 K, $CDCl_3$) δ 1.56 (m, 1H, CH_2), 2.05 (d, $^2J(P,H) = 12.8$ Hz, 3H, PCH_3), 2.33 (m, 1H, CH_2), 3.60 (m, 2H, NCH_2), 3.55−3.90 (m, 8H, OCH_2), 3.90 (m, 2H, NCH_2), 4.50, 4.74 (d_{AB}, superimposed with the *exo* form, 4H, $ArCH_2$), 7.01 (d, $J = 7.0$ Hz, 4H, ArH), 7.24 (m, 2H, ArH), 7.86

(26) Nelson, E. R.; Maienthal, M.; Lane, L. A.; Benderly, A. A. *J. Am. Chem. Soc.* **1957**, *79*, 3467.

Table 5. Crystal Data and Refinement Parameters

	1	**1**·$Hg(SCN)_2$	**2**	**5**	**5**·$LiNO_3$
formula	$C_{22}H_{29}N_2O_3PS$	$C_{24}H_{29}HgN_4O_3PS_3$	$C_{24}H_{33}N_2O_4PS$	$C_{23}H_{31}N_2O_5P$	$C_{23}H_{31}LiN_3O_8P$
temp	18	18	18	18	18
M_r	432.50	749.25	476.57	446.49	515.42
system	orthorhombic	monoclinic	orthorhombic	orthorhombic	orthorhombic
space group	Pbca	$P2_1/n$	$Pnn2$	$Pn2_1a$	$Cmc2_1$
a (Å)	16.471(3)	7.521(1)	12.165(5)	26.968(3)	17.014(2)
b (Å)	9.925(4)	27.322(3)	13.296(2)	12.283(1)	10.870(2)
c (Å)	26.804(8)	14.027(2)	15.380(5)	13.630(2)	13.556(1)
α (deg)	90	90	90	90	90
β (deg)	90	101.25(2)	90	90	90
γ (deg)	90	90	90	90	90
V (Å^3)	4382(2)	2827.0(7)	2488(1)	4514.9(9)	2507.1(5)
D_x (g/cm^{-3})	1.31	1.760	1.27	1.31	1.366
Z	8	4	4	8	4
λ (Å)	0.71069	1.54178	0.71069	0.71069	0.71069
F(000)	1840	1464	1016	1904	1084
μ (mm^{-1})	0.246	3.295	0.226	0.159	0.162
crystal size (mm)	0.21 × 0.25 × 0.15	0.20 × 0.10 × 0.08	0.14 × 0.21 × 0.16	0.3 × 0.4 × 0.4	0.6 × 0.4 × 0.24
$2\theta_{max}$(deg)	52	135	52	55	56
range of hkl	$0 \le h \le 20$	$0 \le h \le 9$	$0 \le h \le 14$	$0 \le h \le 34$	$-22 \le h \le 22$
	$0 \le k \le 12$	$0 \le k \le 32$	$0 \le k \le 15$	$0 \le k \le 15$	$-14 \le k \le 14$
	$0 \le l \le 32$	$-16 \le l \le 16$	$0 \le l \le 18$	$0 \le l \le 17$	$-17 \le l \le 0$
no. of measd reflcns	4286	5082	2545	5415	1632
no. of obsd reflcns					
$[I \ge 2\sigma(I)]$	3009	4201	1309	3212	1454
R	0.057	0.044	0.062	0.052	0.038
R (all data)	0.082	0.052	0.122	0.095	0.045
wR_2	0.175	0.117	0.172	0.085	0.097
$\omega = 1/(\sigma^2(F_o^2) + gP^2 + g'P)$					
g	0.1141	0.0734	0.0972	0.0356	0.0683
g'		4.07			
S	1.02	1.03	0.89	0.97	1.035
Δ/σ	0.01	0.03	0.03	0.01	0.01
$\Delta\rho$(max, min) (e Å^3)	0.49, −0.34	1.65, −1.75	0.32, −0.24	0.22, −0.16	0.20, −0.22

(s, 2H, ArH); ^{13}C NMR (75 MHz, 253 K, $CDCl_3$) δ 16.1 (J = 86.8 Hz, PCH_3), 23.9 (J = 3.7 Hz, CH_2), 52.5 (NCH_2), 69.7, 71.0, 72.0 (OCH_2), 124.3 (ArCH), 125.3 (J = 5.4 Hz, ArCH), 128.6 (J = 4.0 Hz, ArCH), 128.8 (ArCH), 138.2 (J = 1.6 Hz, ArCq), 145.8 (superimposed with the *exo* form, ArCq); ^{31}P NMR (81 MHz, 233 K, $CDCl_3$) δ 70.38.

28-Methyl-8,11,14,17-tetraoxa-1,24,28-diazaphosphatetracyclo[22,3,1,1^{2,6},1^{19,23}]triaconta-2,4,6(29),19,21,23(30)-hexaene 28-Sulfide (2). To a stirred mixture of **7** (300 mg, 0.69 mmol), 1,3-propanediol ditosylate (291 mg, 0.76 mmol), and tetrabutylammonium chloride (71 mg, 0.24 mmol) in toluene (70 mL) was added a solution of NaOH (880 mg, 22 mmol) in water (5 mL). The resultant mixture was heated to 70 °C and vigorously stirred for 4 days. The reaction mixture was cooled to room temperature, and the water layer was extracted with toluene. The combined toluene extracts were washed with water and brine, dried (MgSO4), filtered, and evaporated under vacuum. Silica gel column chromatography (ethyl acetate/dichloromethane 1:9 and then 1:1 as eluent) of the residue afforded **2** (158 mg, 0.33 mmol, 48%) as a white powder: mp 147 °C; ^{1}H NMR (500 MHz, 293 K, $CDCl_3$) δ 1.76 (d, ^2J(P,H) = 13.5 Hz, 3H, PCH_3), 1.93 (m, 1H, CH_2), 2.23 (m, 1H, CH_2), 3.26 (m, 2H, NCH_2), 3.5−3.8 (m, 12H, OCH_2), 4.03 (m, 2H, NCH_2), 4.44, 4.72 (d_{AB}, ^2J(A,B) = 13.4 Hz, 4H, $ArCH_2$), 7.01 (d, J = 7.5 Hz, 2H, ArH), 7.30 (t, J = 8.0 Hz, 2H, ArH), 7.34 (d, J = 8.2 Hz, 2H, ArH), 7.46 (s, 2H, ArH); ^{13}C NMR (5O MHz, 300 K, $CDCl_3$) δ 22.0 (J = 93.7 Hz, PCH_3), 27.0 (CH_2), 49.2 (NCH_2), 70.1, 70.8, 70.9, 72.2 (OCH_2), 124.7 (J = 2.2 Hz, ArCH), 125.8 (J = 4.3 Hz, ArCH), 127.2 (J = 4.1 Hz, ArCH), 129.2 (J = 1.9 Hz, ArCH), 139.2 (J = 2.0 Hz, ArCq), 145.0 (ArCq); ^{31}P NMR (81 MHz, 300 K, $CDCl_3$) δ 81.22; EIMS m/z 477 (M^+). Anal. Calcd for $C_{24}H_{33}N_2O_4PS$: C, 60.49; H, 6.98; N, 5.88; P, 6.50; S, 6.73. Found: C, 60.28; H, 6.95; N, 5.83; P, 6.19; S, 6.64.

25-Methyl-8,11,14-trioxa-1,21,25-diazaphosphatetracyclo[19,3,1,1^{2,6},1^{16,20}] heptacosa-2,4,6(26),16,18,20(27)hexaene 25-Oxide (3). A solution of **8** (103 mg, 0.27 mmol), 1,3-propanediol ditosylate (114 mg, 0.29 mmol), and NaH (27 mg, 0.68 mmol, 60% in oil) in THF (30 mL) was heated under reflux for 2 h. After the reaction mixture was cooled to room temperature, the remaining NaH was destroyed with a minimum amount of water. After evaporation of the solvent, the residue was taken up in CH_2Cl_2 and water. The aqueous layer was extracted with CH_2Cl_2, and the combined organic phases were washed with water and dried over $MgSO_4$. The solvent was evaporated to give an oil which was purified by silica gel column chromatography (acetone/dichloromethane 1:1). **3** was obtained as a white powder (77 mg, 0.18 mmol, 68%) which can be recrystallized from acetone: mp 159 °C; ESI MS m/z 417.7 ($[M + H]^+$), 439.6 ($[M + Na]^+$). Anal. Calcd for $C_{22}H_{29}N_2O_4P$: C, 63.45; H, 7.02; N, 6.73; P, 7.44. Found: C, 63.55; H, 7.11; N, 6.45; P, 7.46.

3-*exo*: ^{1}H NMR (500 MHz, 213 K, $CDCl_3$) δ 1.34 (d, ^2J(P,H) = 14.9 Hz, 3H, PCH_3), 1.58 (m, 1H, CH_2), 2.33 (m, 1H, CH_2), 3.30 (m, 2H, NCH_2), 3.5−4.0 (m, 8H, OCH_2), 4.21 (m, 2H, NCH_2), 4.51, 4.83 (d_{AB}, ^2J(A,B) = 11.7 Hz, 4H, $ArCH_2$), 7.07 (s, 2H, ArH), 7.33 (s, 2H, ArH), 7.41 (s, 2H, ArH), 7.70 (s, 2H, ArH); ^{31}P NMR (81 MHz, 223 K, $CDCl_3$) δ 33.29.

3-*endo*: ^{1}H NMR (500 MHz, 213 K, $CDCl_3$) δ 1.58 (m, 1H, CH_2), 1.61 (d, ^2J(P,H) = 14.3 Hz, 3H, PCH_3), 2.15 (m, 1H, CH_2), 3.5−4.0 (m, 8H, OCH_2), 3.82 (m, 4H, NCH_2), 4.60, 4.70 (d_{AB}, ^2J(A,B) = 13.0 Hz, 4H, $ArCH_2$), 6.95 (d, J = 7.0 Hz, 2H, ArH), 6.99 (d, J = 7.8 Hz, 2H, ArH), 7.26 (s, 2H, ArH), 7.91 (s, 2H, ArH); ^{13}C NMR (50 MHz, 200 K, CD_2Cl_2) δ 7.9 (J = 113.2 Hz, PCH_3), 24.2 (CH_2), 51.6 (NCH_2), 69.3, 70.0, 71.5 (OCH_2), 122.1 (ArCH), 122.2 (ArCH), 124.7 (ArCH), 128.4 (ArCH), 138.2 (ArCq), 144.4 (ArCq); ^{31}P NMR (81 MHz, 223 K, $CDCl_3$) δ 27.61.

28-Methyl-8,11,14,17-tetraoxa-1,24,28-diazaphosphatetracyclo[22,3,1,1^{2,6},1^{19,23}]triaconta-2,4,6(29),19,21,23(30)-hexaene 28-Oxide (4). A solution of **9** (200 mg, 0.48 mmol), 1,3-propanediol ditosylate (201 mg, 0.52 mmol), and NaH (55 mg, 1.38 mmol, 60% in oil) in THF (50 mL) was heated under reflux for 2 h. After the reaction mixture was cooled to room temperature, the remaining NaH was destroyed with a minimum amount of water. After evaporation of the solvent, the residue was taken up in CH_2Cl_2 and water. The aqueous layer was extracted with CH_2Cl_2, and the combined organic phases were washed with water and dried over $MgSO_4$. The solvent was evaporated to give an oil which was purified by

silica gel column chromatography (ethyl acetate/dichloromethane 1:9 and then 1:1). **4** was obtained as a colorless oil (173 mg, 0.38 mmol, 78%) which can be recrystallized from acetone/*n*-hexane: mp 135.5 °C; ^{1}H NMR (500 MHz, 283 K, $CDCl_3$) δ 1.32 (d, ^2J(P,H) = 14.6 Hz, 3H, PCH_3), 2.02 (m, 1H, CH_2), 2.35 (m, 1H, CH_2), 3.65 (m, 4H, NCH_2), 3.62−3.85 (m, 12H, OCH_2), 4.54, 4.58 (d_{AB}, ^2J(A,B) = 12.8 Hz, 4H, $ArCH_2$), 6.93 (d, J = 7.9, 2H, ArH), 7.08 (d, J = 8.0, 2H, ArH), 7.24 (t, J = 7.8, 2H, ArH), 7.76 (s, 2H, ArH); ^{13}C NMR (50 MHz, 300 K, $CDCl_3$) δ 10.6 (J = 114.8 Hz, PCH_3), 26.2 (J = 3.2 Hz, CH_2), 49.8 (NCH_2), 70.4, 70.5, 71.2, 72.4 (OCH_2), 121.7 (J = 4.4 Hz, ArCH), 123.0 (ArCH), 124.5 (J = 2.7 Hz, ArCH), 128.8 (ArCH), 139.2 (ArCq), 145.0 (J = 3.2 Hz, ArCq); ^{31}P NMR (81 MHz, 300 K, $CDCl_3$) δ 24.95; ESI MS m/z 461 ($[M + H]^+$), 483 ($[M + Na]^+$). Anal. Calcd for $C_{24}H_{33}N_2O_5P$: C, 62.60; H, 7.22; N, 6.08; P, 6.73. Found: C, 63.00; H, 7.27; N, 5.98; P, 6.57.

27-Methyl-8,11,14,17-tetraoxa-1,24,27-diazaphosphatetracyclo[22,2,1,1^{2,6},1^{19,23}]nonacosa-2,4,6(28),19,21,23(29)-hexaene 27-Oxide (5). To a stirred mixture of **9** (300 mg, 0.71 mmol) and tetrabutylammonium chloride (100 mg, 0.34 mmol) in 1,2-dichloroethane (72 mL) was added a solution of NaOH (4.1 g, 100 mmol) in water (20 mL). The resultant mixture was heated to 70 °C and vigorously stirred for 1 day. The reaction mixture was cooled to room temperature and the water layer was extracted with toluene. The combined toluene extracts were washed with water and brine, dried with $MgSO_4$, filtered, and evaporated under vacuum. The crude product was recrystallized from acetone/*n*-hexane to give pure **5** (200 mg, 0.45 mmol, 63%) as a beige solid: mp 145 °C; ^{1}H NMR (200 MHz, 300 K, $CDCl_3$) δ 1.85 (d, ^2J(P,H) = 15.1 Hz, 3H, PCH_3), 3.68−4.07 (m, 16H, NCH_2 et OCH_2), 4.53, 4.72 (d_{AB}, ^2J(A,B) = 13.4 Hz, 4H, $ArCH_2$), 6.70 (m, 4H, ArH), 7.25 (t, J = 8.1 Hz, 2H, ArH), 7.97 (s, 2H, ArH); ^{13}C NMR (50 MHz, 300 K, $CDCl_3$) δ 14.2 (J = 114.8 Hz, PCH_3), 42.4 (J = 8.6 Hz, NCH_2), 71.0, 71.1, 71.5, 72.0 (OCH_2), 112.7 (J = 6.9 Hz, ArCH), 114.7 (J = 3.5 Hz, ArCH), 118.9 (ArCH), 129.3 (ArCH), 140.0 (ArCq), 142.1 (J = 8.0 Hz, ArCq); ^{31}P NMR (81 MHz, 300 K, $CDCl_3$) δ 30.33; ESI MS m/z 469.1 ($[M + Na]^+$), 485 ($[M + K]^+$). Anal. Calcd for $C_{23}H_{31}N_2O_5P$: C, 61.87; H, 7.00; N, 6.27; P, 6.94. Found: C, 61.93; H, 7.09; N, 6.31; P, 7.07.

Crystal Structures. Suitable crystals were obtained as follows: for **1**, by slow evaporation from benzene/hexane; for **1**·$Hg(SCN)_2$, the crystals appeared by slow evaporation from a solution of $Hg(SCN)_2$ and **1** in acetonitrile; for **2** by evaporation from a CH_2Cl_2/*n*-hexane solution; for **5** by evaporation from acetone/*n*-hexane; for **5**·$LiNO_3$ by evaporation from a methanol solution of **5** and $LiNO_3$. Crystal data, data collection and refinement parameters are summarized in Table 5. The lattice parameters were refined using a minimum of 15 reflections in 2θ range 5−30°. The measurements were performed with a Huber four-circle diffractometer and a rotating anode equipped with graphite-monochromatized Cu Kα for **1**·$Hg(SCN)_2$ or with a Syntex $P2_1$ diffractometer and Mo Kα radiation for the other data collections. For all data collections, one standard reflection was monitored every 50 measurements; no significant deviation was observed. The structure of **1**·$Hg(SCN)_2$ was solved by Patterson; the four other structures were solved by direct methods with SHELXS86.[27] The structures were refined anisotropically for non-H-atoms using F^2 values with SHELXL93.[28] In each case, the positions of the H-atoms were calculated with AFIX and included in the refinement with a common isotropic temperature factor. For **1**·$Hg(SCN)_2$, two positions (A and B) of the atoms O(8), C(9) of the second independent molecule were refined; the occupation factors converge to 0.57 (position A) and 0.43 (position B) at the end of the refinement.

In **2**, except for the atom pairs C(12), C(13) and C(25), C(27), the molecule has a mirror plane of symmetry passing through P(28), C(26), C(31), S(32) and the midpoint of the C(12)−C(13) bond. Figure 6 shows clearly that C(12), C(13) on one hand, and C(24), C(25) on the other hand are not mirror images of each other so that space group *Pnnm* is excluded.

For the structure of **5**, there are two independent molecules (labeled **a** and **b**) in the asymmetric part of the unit cell. The two molecules adopt a different conformation. In the first one, atoms C(12) and C(13) are disordered; two positions were refined, their occupation factors converge to 0.52 and 0.48.

The structure of **5**·$LiNO_3$ has been refined in the centrosymmetric space group $Cmc2_1$, because all atoms, except C(12), are related by the mirror plane. Two positions have been refined for C(12).

In both cases of disorder, restraints on bond lengths and nonbonded 1−3 distances involving the disordered atoms were applied. Scattering factors were taken from ref 29.

Selected bond distances and angles around the phosphorus atom are compared in Table 3. The final atomic coordinates for the five structures and full lists of bonds distances and angles, anisotropic thermal parameters, and hydrogen atom positions have been deposited with the Cambridge Crystallographic Data Centre.[30]

Acknowledgment. We thank Dr. Pascal Simon[31] and Carmen Esteban-Calderon for preliminary results in early stages of this work. B.T. and J.-P.D. thank the FNRS (Belgium) and the FDS (UCL, Belgium) for financial support.

Supporting Information Available: The ^{1}H NMR spectra for **2**, **3**, **4**, and **5**, the variable-temperature ^{31}P NMR spectra of **1**, and the stereoviews of the X-ray structures of **1**, **1**·$Hg(SCN)_2$, **2**, **5**, and **5**·$LiNO_3$ (10 pages). This material is contained in libraries on microfiche, immediately follows this article in the microfilm version of the journal, and can be ordered from the ACS; see any current masthead page for ordering information.

JO961206E

(27) Sheldrick, G. M. *SHELXS86*, Program for the Solution of Crystal Structures.; University of Göttingen, Göttingen, Germany, 1985.

(28) Sheldrick, G. M. *SHELXL93*, Program for Crystal Structure Refinement; University of Göttingen, Göttingen, Germany, 1993

(29) *International Tables for X-ray Crystallography*; Kynoch Press: Birmingham, England, 1974; Vol. 4.

(30) The authors have deposited atomic coordinates for these structures with the Cambridge Crystallographic Data Centre. The coordinates can be obtained, on request, from the Director, Cambridge Crystallographic Data Centre, 12 Union Road, Cambridge, CB2 1EZ, UK.

(31) Simon, P. Doctoral Thesis, Université J. Fourier, Grenoble, France, 1989.

(32) Motherwell, W. D. S.; Clegg, W. *PLUTO, Program for Plotting Molecular and Crystal Structures*; University of Cambridge, Cambridge, England, 1978.

(33) Johnson, C. K. *ORTEP II*; Report ORNL-5138; Oak Ridge National Laboratory, Tenessee, Oak Ridge, TN, 1976.